

## Anisotropy of the Electronic Work Function of Metals

R. SMOLUCHOWSKI\*

*Palmer Physical Laboratory, Princeton University, Princeton, New Jersey*

(Received July 24, 1941)

Work function is experimentally known to be different for different faces of a crystal by amounts ranging from one-tenth to half a volt. For tungsten the faces can be arranged according to decreasing work function as follows: 110, 211, 100 and finally 111. The explanations so far suggested for the differences of the work function are discussed and shown to give either an incorrect sequence or a wrong order of magnitude of the observed differences. The author uses the picture of Wigner and Bardeen according to which the work function is a sum of a volume contribution and a contribution due to a double layer on the surface of the metal. The origin of the latter can be described in the following manner. With every atom one can associate a polyhedron ("s-polyhedron") with the atom at its center, such that it contains all points nearer to the atom under consideration than to any other atom. If the distribution of the electron density within these polyhedra of the surface atoms was the same as for the inside atoms then there would be no double layer on the surface. However, this is not the case since the total energy is lowered by a redistribution of the electron cloud

on the surface. There are two effects: the first is a partial spread of the charge out of the s-polyhedra and the second is a tendency to smooth out the surface of the polyhedra. In consequence of the second effect the surfaces of equal charge density are more nearly plane than in the original picture. The two effects have opposite influences and since they are comparable in magnitude, it is not possible to predict the sign of the total double layer without numerical computations. Some general formulae for the double layers are derived and discussed more fully in the case of a simple cubic and a body-centered cubic lattice. The minimum problem of the surface energy is solved for four faces of a body-centered crystal and the results are applied to the case of tungsten. One obtains the differences between the work functions for different directions. The results agree satisfactorily with the experimental data: assuming a reasonable density of the free electrons, one obtains the correct sequence of faces and the correct differences of the work function. The surface energies are calculated and found in agreement with the observed stability of certain crystal faces.

### 1.

THE intensity of thermionic electron emission of metals is well represented as a function of temperature by the formula

$$I = AT^2 e^{-\varphi/kT}, \quad (1)$$

where  $A$  and  $\varphi$  are constants. Many experimental investigations have shown that this emission is anisotropic. In particular the work function  $\varphi$ , representing the minimum energy necessary to bring an electron from the inside of the metal to the outside, is different for different crystal faces.<sup>1</sup> Recent photographs<sup>2</sup> of emission of single crystalline spheres of various metals give a nice

illustration of this fact. They indicate also that the directional dependence of the work function is mainly connected with crystallographic orientation of the surfaces, and is the same for two metals if the metals have the same crystal lattice.

The purpose of this paper is to give a theoretical explanation for the observed differences of  $\varphi$ . A few explanations have already been suggested. One of them assumes an anisotropic Fermi surface inside the metal which would lead to different values of the work function for different directions. It will be explained below why this idea appears to us to be incorrect.

Let us consider the  $k$  space which for electrons in a metal is similar to the momentum space for free electrons. The difference is that, in general, the energy is not proportional to  $k^2$ . This  $k$  space is, as is well known, divided into regions, the so-called Brillouin zones, within which the energy varies continuously. To illustrate this we use a simple two-dimensional  $k$  lattice. We assume first (Fig. 1(a)) that the Fermi surface,  $A$  (that is the equi-energetical surface corresponding to

\* Now at General Electric Company Research Laboratory, Schenectady, New York.

<sup>1</sup>R. P. Johnson and W. Shockley, *Phys. Rev.* **49**, 436 (1936); R. B. Nelson, M. I. T. Thesis 1938; S. T. Martin, *Phys. Rev.* **56**, 947 (1939); M. H. Nichols, *Phys. Rev.* **57**, 297 (1940). A probably more correct definition of work function is: the temperature independent term of the work required to remove an electron from the metal. The influence of temperature on the work function, if any, is still an unsolved problem. [See, e.g., C. Herring, *Phys. Rev.* **59**, 889 (1941)].

<sup>2</sup>M. Benjamin and R. O. Jenkins, *Proc. Roy. Soc.* **176**, 262 (1940).

the energy  $E_0$  of the highest occupied electron states), lies within one zone and does not touch nor cross any zone boundary. One computes the number of electrons having momentum components in a particular direction larger than a certain minimum value  $p_0$ . The maximum energy of electrons in every direction is, by definition of the Fermi surface, the same. Thus  $p_0$  and therefore the work function  $\phi$  is isotropic. Let us consider now the other case (Fig. 1(b)) in which the Fermi surface touches or crosses the zone boundary. As we know there is a region of forbidden energy values at the zone boundary. Thus from the energy spectrum of the electrons having enough energy to leave the metal certain regions are missing and the electron emission intensity, therefore, is lower. The minimum energy necessary to bring out an electron is now no longer isotropic. In formula (1) the factor  $A$  would be multiplied by  $(1-r)$  where  $r$  is the so-called reflection coefficient. (For polycrystalline material an "average" reflection coefficient  $\bar{r}$  occurs.) Since the energy discontinuity occurs at, or at least near, the Fermi surface, the number of electrons missing from the emission depends upon temperature. Therefore the ratio of the number of missing electrons to the total current is not constant. This would amount to a temperature dependent reflection coefficient  $r(T)$ . The experimental data,<sup>1</sup> however, are, within the limits of error, well represented with a constant  $r$ , different for each surface. From the Richardson plots we get the work functions  $\phi$ . Certain special aspects of the experimental data and the so-called "patch-effect" were discussed in this connection by Nichols.<sup>3</sup> If the emission were disturbed by such a boundary as discussed above, then one would not obtain a straight Richardson line. We are thus led to the conclusion that either such crossings of the Fermi surface and the zone boundary do not occur or their influence is covered up completely by electrons occupying other zones. If  $dr/dT$  is small it may not show up in the Richardson plot because of the exponential term. As we know there is a very complicated system of zones in metal lattices and electrons can originate in more than one zone.

<sup>3</sup> M. H. Nichols, Rev. Mod. Phys. (to appear shortly).

Also, if such crossings were responsible for the anisotropy, there would be no reason for metals crystallizing in the same crystal lattice to have a similar anisotropy as is true for tungsten and molybdenum.

Frequently one has to assume a certain  $r \neq 0$  in order to fit the experimental data. This is probably connected with some surface phenomena, which we do not consider here. All we are interested in now is the work function and

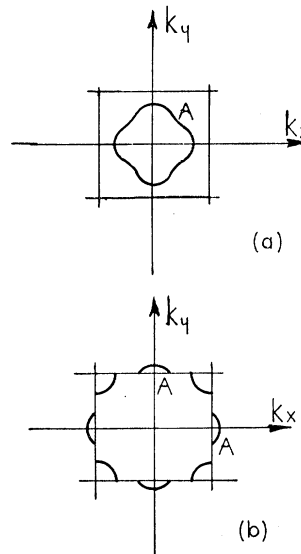


FIG. 1.  $k$  space of a two-dimensional cubic lattice with the Fermi surface (a) contained within one zone (b) crossing the boundary.

the fact that its anisotropy cannot be attributed to a volume effect. In other words, the presence of an accidental anisotropy of the Fermi surface is not supported by experiment. The anisotropy of the work function and the necessity for assuming  $r \neq 0$ , if  $A$  is a general constant, must have another origin.

It is perhaps worth including a remark, which is, however, not an essential point in our considerations. Suppose the Fermi surface in a certain direction, say the  $x$  direction, falls just within the forbidden region. One might conclude that the electron emission in that direction is impossible. This is erroneous, since one has to consider the fact that the connection between  $k$  and  $E$  is not unique. If the zone boundary occurs at  $k_x = k$ ,  $k_y = k_z = 0$  and  $E(k)$  is below the necessary limit then another vector  $k(k_x, k_y, k_z)$  may exist lying within the zone, such that its momentum along the  $x$  direction is large enough to bring the electron out from the metal.

Müller<sup>4</sup> and Benjamin and Jenkins<sup>2</sup> made calculations on the hypothesis that the condition of the Bragg reflection of the electron wave is fulfilled for those electrons which have enough energy to escape across a particular crystal face. As pointed out by the last authors, this hypothesis leads to impossibly high energy values for the electrons and has some further drawbacks.

In the present paper we want to correlate the observed facts on the basis of another idea brought forward by Wigner and Bardeen.<sup>5</sup> According to these authors the work function is essentially a sum of two parts; the first is the volume contribution arising from the binding energy of the electron in the metal as a whole and the second is the energy necessary to penetrate the double layer at the surface. The first part is isotropic and is equal to the difference of the energy of a crystal composed out of an equal number of positive and negative charges and of the same crystal containing one electron less. It has been evaluated for a free electron model by these authors. Later Bardeen<sup>6</sup> made a careful study of the double layer using self-consistent solutions of the Fock equations. The model used by Bardeen consists of a charge distribution which is uniform positive inside of the crystal and zero outside. The electronic charge distribution, obtained by solving the corresponding Fock equations, is found to be uniform throughout the crystal except in the neighborhood of the surface. There it changes slowly and decreases to zero outside of the crystal within a fraction of the lattice constant from the surface. We have thus a deviation of the electronic density from the distribution characteristic for the inside of the metal and a spread of the charge beyond the surface of the crystal. From the point of view of the work function this is equivalent to the presence of a double layer which the electrons have to penetrate on their way to the outside.

The model in which the positive charge has a uniform distribution is of course isotropic and it is only if the atomic structure of the positive charges is taken into account that any anisotropy can be expected. Even in this latter

model the volume contribution will remain isotropic and it is the double layer which must be made responsible for the observed differences in the work function or the potential differences<sup>7</sup> between different crystal faces.

The moment of the double layer on the surface of a metal is defined as the electrostatic potential difference between the outside of the metal and a point inside. Every atom in the lattice can be surrounded by a polyhedron of which each point is nearer to the atom under consideration than to any other one. These polyhedra are called usually *s*-polyhedra and the spheres of equal volume surrounding the atoms *s*-spheres. The inside point, in the definition of the double layer, is chosen at the surface of the *s*-sphere surrounding some atom. The point outside is taken as usual at a distance large compared with the lattice parameter and small compared with the size of the crystal surface. If all the atoms including those at the surface had the same radial electronic distribution inside the *s*-spheres, there would be no double layer since the dipole moment of an *s*-sphere is zero. However, because in the neighborhood of the surface atom the charge distribution is appreciably disturbed, a double layer may result.<sup>8</sup> If the double layer has a moment *M* normal to the surface and if we define its sign as positive if the positive charge is on the outside and the negative on the inside of the surface then the work function is given by

$$A - 4\pi eM,$$

where *A* is the volume contribution mentioned before.

For a continuous positive charge distribution the double layer is zero if the negative charge density is constant within the metal and zero outside.

## 2.

We wish to carry out first a general qualitative, and later on a quantitative investigation of the conditions which occur on the surface of the metal and to see how they depend upon the

<sup>4</sup> E. Müller, *Naturwiss.* **27**, 820 (1939).

<sup>5</sup> E. Wigner and J. Bardeen, *Phys. Rev.* **48**, 84 (1935).

<sup>6</sup> J. Bardeen, *Phys. Rev.* **49**, 653 (1936).

<sup>7</sup> H. E. Farnsworth and B. A. Rose, *Proc. Nat. Acad. Sci.* **19**, 777 (1933); B. A. Rose, *Phys. Rev.* **44**, 585 (1933).

<sup>8</sup> See F. Seitz *Modern Theory of Solids* (McGraw-Hill Book Company, New York, 1940), p. 396.

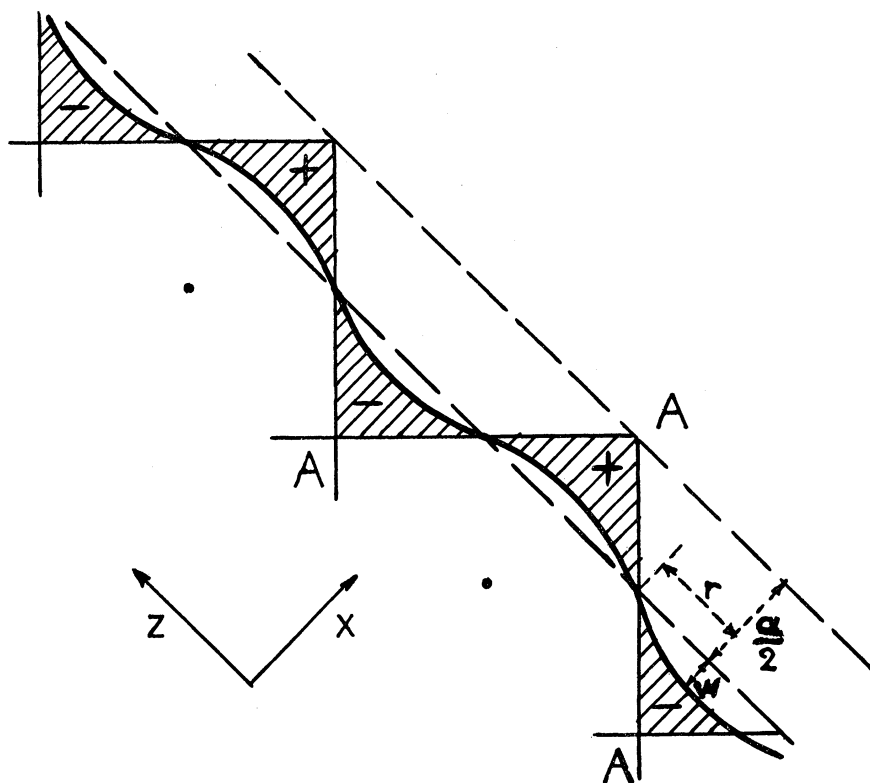


FIG. 2. Positive double layer resulting from the smoothing effect. Thick line represents the equilibrium charge distribution.

orientation of this surface with respect to the crystal lattice. Let us imagine a crystal surface which has just been exposed by splitting the crystal into two. If no changes of the charge distribution of the surface atoms occur then according to our definition there would be no double layer. However, we might expect two effects. First, as a result of the absence of the next atomic layer the potential field acting on the electrons binds them less than the potential in the inside of the metal. Thus the wave functions of these electrons are less concentrated within the original *s*-polyhedra; their expansion into the free space is accompanied by a decrease of the energy. This spread should be comparable with the difference of atomic diameter in crystal and vapor state. Because of this spreading of the negative charge there arises a corresponding positive charge within the *s*-polyhedra. We have thus a negative double layer which increases the work function since it is an additional potential

preventing the electrons from leaving the crystal. We shall consider this effect later more in detail.

The other effect occurring on the surface is the smoothing of the surface of the electronic cloud of the metal. This smoothing is due to the fact that the energy of electrons when enclosed in a volume bounded by large flat planes is lower than when surrounded by the complicated walls of the surface polyhedra (Fig. 2). It means that the charge "flows" from the "hills" into the "valleys" formed by the surface atoms. In this way there arises a net positive charge on the "hills" and a negative charge in the "valleys." This is a positive double layer. The potential drop here decreases the work function. Thus the less smooth the final surface the more difficult it is for the electrons to leave the metal. The electrostatic energy accompanying the smoothing-out limits this process. The final shape of the surface of the electron cloud will be something like the thick curve in Fig. 2. It corresponds to

the balance between the different processes. The first effect mentioned above we shall call "spreading," the second "smoothing." They are both associated with the decrease of energy and are really not independent. However, since they have opposite influence on the work function it is convenient in a qualitative discussion to consider them separately.

We shall derive now some general formulas governing both effects making use of a very simple model. Let us consider first the spreading effect in the case of a uniform distribution of negative and positive charges in *s*-polyhedra throughout the whole crystal. In Fig. 3 the ordinate is the charge density  $\sigma$  (both + and -) per unit volume, the line *P-P* is the surface of the metal and at the same time the surface of the uniform charge distribution in the original crystal. We assume now that the electronic charge spreads so that its density decreases linearly to zero. One can see that this approximation is justified by comparing it with the exact distribution as calculated by Bardeen for a particular case. Thus up to the point *S* the negative and positive charges compensate each other. From *S* to *P* we have positive charge increasing up to the density  $\frac{1}{2}\sigma$  on the inner side of the surface and then a negative charge decreasing from *P* to *N* in a symmetric distribution. If the spread of the electronic charge is small so that the disturbance does not reach the centers of the *s*-polyhedra then the potential difference is given by

$$D = -\frac{2\pi\sigma}{3} \frac{y^2}{e}$$

We introduce *n*, the number of electrons in a unit cell, and put for the lattice constant *d* its value *b* expressed in atomic units:

$$D = -\frac{n}{b} \left(\frac{y}{d}\right)^2 \cdot 56.8 \text{ ev.} \quad (2)$$

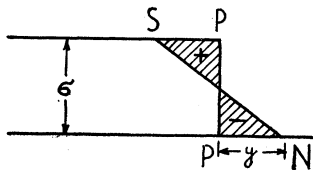


FIG. 3. Spreading of the electron density and the resulting negative double layer.

If however the disturbance of the negative charge in the metal extends beyond the center of the surface polyhedra then the positive charges in these polyhedra will be displaced towards the surface, by the amount  $\frac{1}{2}d + y - (2dy)^{\frac{1}{2}}$ . Then the potential drop is given by

$$D = -\frac{2\pi ne^2}{3} \frac{1}{d} \left[ \left(\frac{y}{d}\right)^2 - \frac{3}{d^2} [d - (2dy)^{\frac{1}{2}}]^2 \right]. \quad (3)$$

Both formulas give the value of the double layer on a flat surface for a uniform charge distribution within the metal.

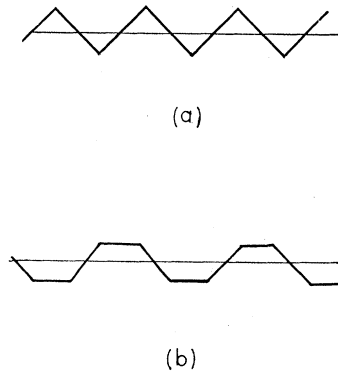


FIG. 4. Cross section of a "pyramidal" and "truncated" charge distribution on the surface.

Let us consider next the smoothing effect on crystal surfaces. In most cases one finds that the profile of the original, "rough," crystal face is either like Fig. 4(a) or 4(b). The plane *P* parallel to the crystal face and equally distant from the "hills" and from the "valleys" is the ideal plane surface which would be obtained if the smoothing were complete. The amount of negative charge "cut off" by this plane is equal to the charge needed to fill up the "valleys." This is a general statement true for all faces. The density of both + and - charges at this plane is  $\frac{1}{2}\sigma$ , half the value of the density inside of the crystal. A coordinate system is chosen so that the axis *x* is normal to the plane *P* and the charge density per unit volume is plotted as a function of *x*. Averages over the whole crystal face are taken parallel to the plane *P*. If the face is made out of prisms parallel to the crystal face (as all *hk0* faces in simple cubic lattices are) the charge is a linear function of *x*. For pyramids it is a quadratic function. Figure 4(b) corresponds to trun-

cated pyramids typical for many faces of body-centered lattices. Typical charge distributions are shown in Fig. 5.

Let  $\frac{1}{2}a$  be the distance from the plane  $P$  to the top of the "hill." We can calculate the potential differences obtained if the face is smoothed out completely, i.e., for all negative charge from the "hills" moved into the "valleys." In the general case of a truncated pyramid the

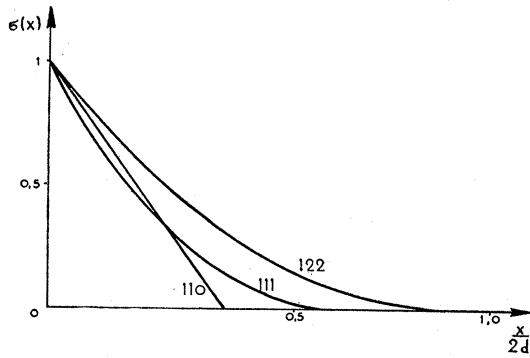


FIG. 5. Average charge density as a function of the distance from the ideal smooth surface for a simple cubic lattice.

charge distribution in the direction perpendicular to the plane  $P$  is given by

$$\sigma(x) = \frac{\sigma}{2a^2}(px^2 - qa/x + a^2)$$

for which the charge density at  $x = \pm \frac{1}{2}a$  is equal to

$$\sigma' = \left(\frac{p}{4} - \frac{q}{2} + 1\right) \frac{\sigma}{2} = m \frac{\sigma}{2}$$

The corresponding potential difference is given by

$$V = \frac{\pi a^2}{2} e \sigma \left(\frac{p}{8} - \frac{q}{3} + 1\right) = \frac{\pi n}{2} \left(\frac{a}{d}\right)^2 \frac{e^2}{d} \left(\frac{p}{8} - \frac{q}{3} + 1\right). \quad (4)$$

For a quadratic decrease of charge density to zero at  $x = \pm \frac{1}{2}a$ :  $m=0$ ,  $p=2q-4$  or for a pyramid  $p=q=4$ ; for a linear decrease to  $\sigma'$  at  $x = \pm \frac{1}{2}a$ :  $p=0$ ,  $q=2(1-m)$  and finally for linear decrease to zero at  $x = \pm \frac{1}{2}a$ :  $m=p=0$ ,  $q=2$ . We shall make frequent use of these formulas for particular cases.

3.

In the former paragraph the effects occurring on the surface were discussed qualitatively and some general formulas were derived. Some particular cases will be considered here in more detail. Although the few metals for which data are available crystallize in a body-centered lattice we shall begin with a brief discussion of the simple cubic lattice. This case provides a good illustration of our model and of the method of approach.

In the simple cubic lattice the 100 face is smooth (Fig. 6). Thus there occurs only the spreading effect; the resulting double layer increases the work function. Next let us consider a  $hk0$  plane (Fig. 6) for which  $a = dhk / (h^2 + k^2)^{1/2}$  and, in formula (4),  $p=m=0$ . We have thus

$$V = \frac{\pi e \sigma}{6} d^2 \frac{h^2 k^2}{h^2 + k^2} \quad (5)$$

for the potential difference which is obtained for complete smoothing. Similarly for a  $hkl$  plane for which

$$a = 2dhkl / (h^2 k^2 + k^2 l^2 + l^2 h^2)^{1/2}$$

and  $m=0$  we get

$$V = \frac{\pi e \sigma}{3} d^2 \frac{h^2 k^2 l^2}{h^2 k^2 + k^2 l^2 + l^2 h^2}. \quad (6)$$

If the smoothing is not complete, there remains

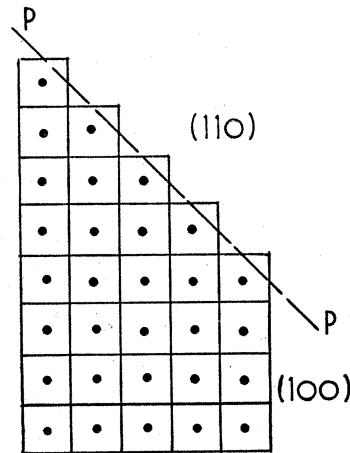


FIG. 6. Simple cubic lattice. Smoothing occurs on the 110 plane, none on the 100 plane.

a certain wave-like surface of the negative charge distribution and a correction should be made. This corrective term has to be subtracted from the values obtained from (5) or (6). We shall give an estimate for this correction below for the body-centered lattice. It is evident, however, that the number  $n$  of electrons per unit cell will enter into the result. Since it occurs as a linear factor it changes only the absolute values and not the relative magnitudes of the double layers for different faces. This is fortunate since  $n$  is unknown for most metals.

Let us consider the body-centered lattice. The polyhedron surrounding each atom in a body-centered crystal lattice is a truncated octahedron (Fig. 7) made out of eight 111 hexagons and six 100 squares. Since there are two atoms per unit cell the volume of the polyhedron is  $\frac{1}{2}d^3$ . We shall consider only a few particular faces which are actually observed on single crystals of tungsten, molybdenum etc. for which experimental data are known. These are the 100, 110, 111 and 211 faces. The structure of these surfaces can be seen in Fig. 8. The most densely packed surface is the 110 face, for which  $a = \sqrt{2}d/4$ ; then comes the 100 face with  $a = \frac{1}{2}d$  and 111 with  $a = \sqrt{3}d/3$ . The 211 face differs greatly from the other three faces which have a (truncated) pyramidal structure. On these faces each atom has at least four nearest neighbors; in the 211 face, on the other hand, an atom has only three nearest neighbors: and out of these two are in the surface layer. Thus there exists a long row of closely packed atoms separated by

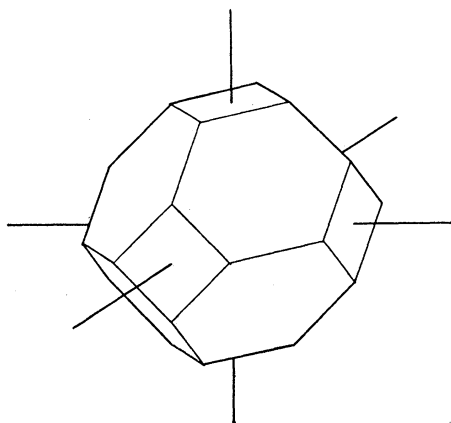


FIG. 7.  $s$ -polyhedron for a body-centered cubic lattice.

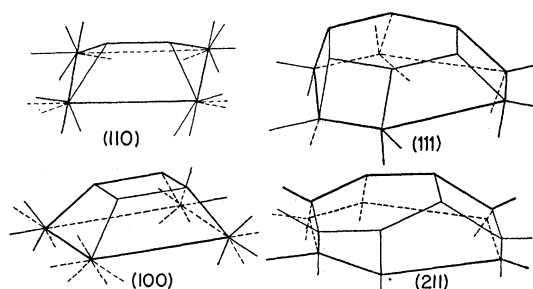


FIG. 8. Charge distribution on different faces of a body-centered cubic lattice.

deep and long depressions.<sup>9</sup> If we consider the atoms on the 211 plane individually then  $a = \sqrt{6}d/4 \cong 0.61d$ . However, if we treat rather the rows of atoms as elements of that surface and average the charge distribution in the  $\bar{1}11$  direction then  $a \cong 0.42d$ . On the 211 plane, the ideal smooth surface, i.e., the plane  $P$ , cuts off certain volumes which fit into the remaining depressions. The charge distributions along the axis  $x$ , perpendicular to the plane  $P$ , are represented in Fig. 9 by continuous lines. For the 100, 110 and 111 faces the charge is a quadratic function of  $x$ , for the 211 face it is linear up to  $x = \frac{1}{6}a$  then quadratic till  $x = \frac{1}{3}a$  and finally again quadratic, with other constants, till  $x = \frac{1}{2}a$ .

We apply now formula (4) and obtain the values of the potential differences as if the smoothing were complete. We express the lattice constant in atomic units  $d = ba_0$ . For the 110 plane we have  $m = 0$ ,  $q = 3$ , and thus

$$V^{110} = \frac{\pi n}{b} \frac{1}{64} \frac{e^2}{a_0} \frac{n}{b} = -1.33 \text{ ev} \quad (7)$$

for the 100 plane  $p = 1$ ,  $q = 2$  and

$$V^{100} = \frac{\pi n}{b} \frac{11}{192} \frac{e^2}{a_0} \frac{n}{b} = -4.88 \text{ ev} \quad (8)$$

for the 111 plane  $p = \frac{4}{13}$ , and  $q = \frac{16}{13}$  and

$$V^{111} = \frac{\pi n}{b} \frac{19}{156} \frac{e^2}{a_0} \frac{n}{b} = -10.38 \text{ ev.} \quad (9)$$

The 211 plane has a rather complicated charge

<sup>9</sup> See S. T. Martin (reference 1), p. 957 or D. Langmuir and R. B. Nelson, *Rev. Sci. Inst.* **11**, 295 (1940).

distribution and the potential difference can be calculated by applying formula (4) separately to each interval within which the charge variation is expressed by a simple formula. The result is

$$V^{211} = \frac{\pi n}{b} \frac{41}{64 \times 9} \frac{e^2}{a_0} = \frac{n}{b} = -6.06 \text{ ev.} \quad (10)$$

If we assume the charge distribution on the 211 face averaged in the  $\bar{1}11$  direction, then we have

$$V^{211'} = \frac{n}{b} = -5.80 \text{ ev.} \quad (11)$$

All these values correspond to an ideal smooth charge distribution. Since, as mentioned before, some of the original structure of the surface will be left over we must correct for this fact. As it will appear later, these corrections are very essential, the surface charge distribution being far from smooth.

4.

So far we have considered the double layers arising on the crystal surfaces as if the smoothing were complete. Now we want to evaluate the actual electron distribution at the surface and the remaining "roughness" of the charge density. In the qualitative discussion it was pointed out that both spreading and smoothing are due to the decrease of kinetic energy of the electron gas, and are limited by the increasing potential energy of the resulting double layers. We shall treat now this question as a variational problem. The kinetic and the potential energy has to be expressed as a function of two parameters, one correlated with the spreading, the other with

the smoothing effect. The total energy per unit surface has to be minimized with respect to each of these two parameters for each surface of the crystal. The calculations are rather involved and we shall consider more in detail only the 211 face which is the easiest to treat.

The charge distribution on the 211 face is rather complicated (see Figs. 8 and 9) and we shall simplify it somewhat. It was said before that on that face the atoms form closely packed rows divided by relatively wide gaps. The approximation we want to use is that of a prismoidal charge distribution similar to that on the 110 face of a simple cubic lattice. However, the angle of the prism is here not a right angle. The width,  $2r$ , of the base of a prism cut off by the  $P$  plane is equal to half the distance between the rows of atoms. The height  $\frac{1}{2}a_{\text{eff}}$  is such that the prism contains the same amount of charge as the part of the  $s$ -polyhedron cut off by the plane  $P$ . The charge density depends thus only upon two coordinates:  $x$ —perpendicular to the surface and  $z$ —lying in the surface and perpendicular to the rows of atoms. In Fig. 10 we have the density plotted against the two coordinates. In the original distribution both charges fill up the prism  $AAA$  with uniform density. The electrons tend to form a more smooth surface along the  $BBB$  line and finally spread along the  $x$  axis. The final charge density is given by the surface  $CCC$ . We put the origin of the coordinates at the point  $B$  and express the electron density in the region  $0 < z < 1$  by

$$\rho = \frac{1}{2}\sigma e^{-\alpha(x-\beta z)} \quad \text{for } x > 0 \text{ and by} \quad (12a)$$

$$\rho = \frac{1}{2}\sigma(2 - e^{\alpha(x-\beta z)}) \quad \text{for } x < 0. \quad (12b)$$

$\sigma$  is here the number of electrons per unit volume inside the crystal, obviously  $\alpha$  is the parameter associated with the spreading effect and  $\beta$  with the smoothing effect. For the original distribution we have  $\beta = a_{\text{eff}}/2r$  and  $\alpha \rightarrow \infty$ . If the smoothing is complete we have  $\beta = 0$ . The charge distribution as given by (12) is convenient for the computation of the kinetic energy. For mathematical reasons a slightly different, essentially equivalent form will be used for the calculation of the potential energy of the double layer. In calculating the kinetic energy it is useful to employ an expression which depends upon the

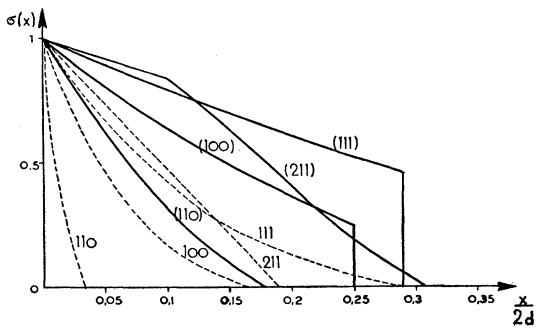


FIG. 9. Average charge density as a function of the distance from the ideal smooth surface for a body-centered cubic lattice.

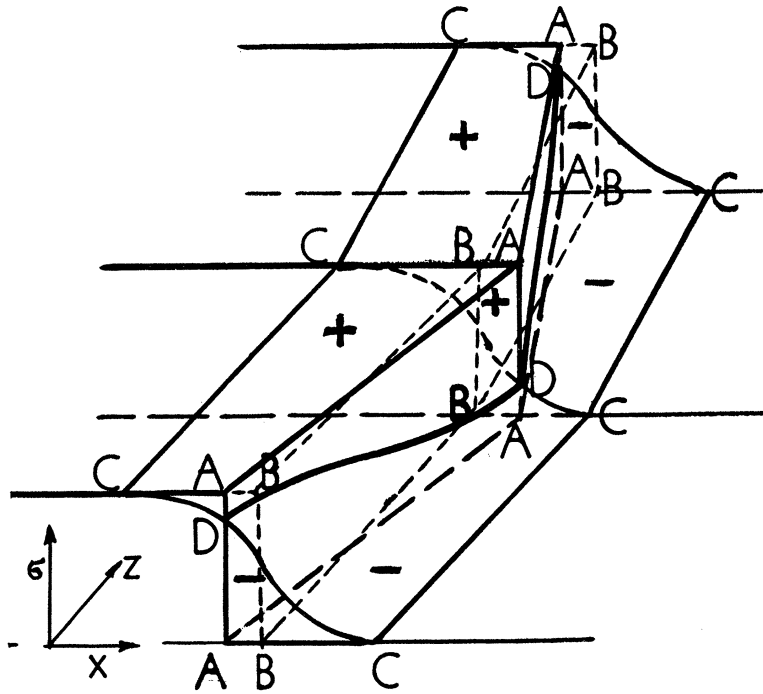


FIG. 10. Spreading and smoothing effect on the 211 face. AAA—original distribution of electron density, CCC—final distribution.

gradient of the density since this is an important magnitude in our considerations. Such an expression was given by Weizsäcker.<sup>10</sup>

$$\text{K.E.} = A\rho^{5/3} + B\frac{(\text{grad}\rho)^2}{\rho} \quad (13)$$

with

$$A = \frac{4\pi\hbar^2}{5m} \left(\frac{3}{8\pi}\right)^{5/3} \quad \text{and} \quad B = \frac{\hbar^2}{32\pi^2m}.$$

The first term is the usual Fermi energy per unit volume, the second term is the important

term depending upon the gradient of charge density. One has to calculate separately for  $x < 0$  and for  $x > 0$ , integrate and add both energies. Integrating from  $x = 0$  to  $-\infty$  with (12b) would give infinity but since we need only the differences of the kinetic energy it is enough to calculate the kinetic energy of the charge which is missing from the continuous distribution for  $x < 0$ . We have thus

$$-\sigma^{5/3} \int_{-\infty}^0 \left\{ \left(1 - \frac{1}{2}e^{\alpha(x-\beta z)}\right)^{5/3} - 1 \right\} dx,$$

which is the decrease of kinetic energy as compared with the original distribution. We can represent the integrand as a series

$$\int_{-\infty}^0 \sum_{k=1}^{\infty} \binom{5/3}{k} \frac{(-1)^k}{2^k} e^{k\alpha x} dx$$

and obtain

$$\frac{1}{\alpha} \sum_{k=1}^{\infty} \binom{5/3}{k} \frac{(-1)^k}{k2^k} = \frac{1}{\alpha} \int_0^{1/2} \frac{(1-u)^{5/3} - 1}{u} du,$$

which can be evaluated. The total kinetic energy per unit length is

$$\sigma^{5/3} A \frac{6r}{2^{5/3}\alpha} - \sigma^{5/3} A \frac{1.5852r}{\alpha} + \sigma B \alpha (1 + \beta^2) 2r \ln 2. \quad (14)$$

<sup>10</sup> C. F. von Weizsäcker, Zeits. f. Physik **96**, 431 (1935).

The first term is the Fermi energy for  $x > 0$ , the second the same for  $x < 0$  and the third "the Weizsäcker energy" due to the gradient of density.

To calculate the potential energy we make a small change in the expression for density so that the potential for the given charge is easy to obtain. We must compute the potential energy of the negative charge outside of the original  $s$ -polyhedron and the same amount of the positive charge inside of the polyhedron. This is shown by the thickly drawn lines in Fig. 10. The charge density along the surface of the polyhedron is given by the line  $DDD$ . Our new distribution differs by replacing this line by a cosine curve and plotting it in a plane perpendicular to the  $x$  axis. We put the origin of the coordinates at the point  $A$ , which is more convenient than point  $B$  for this computation. The charge for  $x > 0$  is now negative, for  $x < 0$  positive. We put

$$\begin{aligned} \rho &= M \cos(\pi z) \int_{-\infty}^{+\infty} \frac{\cos \alpha x \omega}{1 + \omega^2} d\omega + N \int_{-\infty}^{+\infty} \frac{\alpha \omega \sin \alpha x \omega}{1 + \omega^2} d\omega \\ &= M \cos(\pi z) \pi e^{-\alpha|x|} + N \pi \alpha e^{-\alpha|x|} \operatorname{sgn} x \end{aligned} \quad (15)$$

( $\operatorname{sgn} x$  stands for "signum  $x$ ," the sign  $+$  or  $-$  of  $x$ ) which is shown in Fig. 11. The charge has a pattern, in the  $P$  plane, as given in Fig. 12(a). High negative and low positive charge density is indicated by full lines and the opposite by dotted lines. Formula (15) represents well our charge distribution (Fig. 10) and from it the potential can be obtained easily:

$$\begin{aligned} -\frac{V}{4\pi} &= M \cos(\pi z) \int_{-\infty}^{+\infty} \frac{\cos \alpha x \omega}{(1 + \omega^2)(\pi^2 + \alpha^2 \omega^2)} d\omega + N \int_{-\infty}^{+\infty} \frac{\sin \alpha x \omega}{(1 + \omega^2)\alpha \omega} d\omega \\ &= M \cos(\pi z) \frac{1}{\alpha^2 - \pi^2} (\alpha e^{-\pi|x|} - \pi e^{-\alpha|x|}) + N \frac{\pi}{\alpha} (1 - e^{-\alpha|x|}) \operatorname{sgn} x. \end{aligned} \quad (16)$$

The coefficients  $M$  and  $N$  must be adjusted so as to correlate the charge distribution given by (12) with that given by (15). It turns out that we must put

$$M = \frac{e\sigma}{2\pi} (e^{\alpha c} - 1) \quad \text{and} \quad N = \frac{e\sigma}{2\pi\alpha}$$

with  $c = \frac{1}{2} a_{\text{eff}} - r\beta$ . The product  $r\beta = W$  determines the remaining roughness of the surface measured perpendicular to the plane  $P$ . Equation (15) has also the advantage as compared with (12) that the subsequent integration is easy. We have

$$-\int_0^1 dz \int_{-\infty}^{+\infty} dx \frac{V\rho}{4\pi} = M^2 \frac{\pi(2\alpha + \pi)}{2\alpha(\pi + \alpha)^2} + N^2 \frac{\pi^2}{\alpha}$$

and the potential energy per unit length, in proper units has the form

$$\text{P.E.} = \frac{e^2 \sigma^2}{\alpha} \frac{2\alpha + k}{(k + \alpha)^2} r^2 [1 + e^{\alpha c} (e^{\alpha c} - 2)] + \frac{e^2 \sigma^2}{\alpha^3} 2r^2 k \quad (17)$$

with  $k = \pi/2r$ .

The equations of the minimum problem are obtained by differentiating the total energy with respect to  $\alpha$  and  $\beta$  (or  $W$ ). One gets

$$e^m e^{2y} - e^y + \gamma e^{-m} y = 0 \quad (18)$$

with

$$\gamma = \frac{B(\alpha + k)^2 2 \ln 2}{\sigma e^2 r^3 (2\alpha + k)}, \quad m = \frac{\alpha a_{\text{eff}}}{2} \quad \text{and} \quad y = -\alpha\beta r$$

and

$$a_2x^7 + 3ka_2x^6 + (a_1 + 3k^2a_2)x^5 + (3ka_1 + k^3a_2 - 4a_3)x^4 + (3k^2a_1 - 9ka_3)x^3 + (a_1k^3 - 19a_3k^2)x^2 - 18k^3a_3x - 6k^4a_3 + 4a_3ce^{xc}(e^{xc} - 1)x^5 + 2a_3[(3kc - 2)e^{2xc} - (3kc - 4)e^{xc}]x^4 - ka_3[(2kc + 3)e^{2xc} - (2kc + 6)e^{xc}]x^3 - k^2a_3e^{xc}(e^{xc} - 2)x^2 = 0 \quad (19)$$

with  $x = \alpha$  and  $a_1 = \sigma^3 A 1.147$ ;  $a_2 = B(1 + \beta^2)2 \ln 2$  and  $a_3 = \sigma e^2 r$ .

No analytic form of the solution of these equations can be given but a solution is easily obtained by a trial and error method. We get thus  $\alpha$  and  $\beta$  (or  $W = r\beta$ ).

Next we give a brief summary of the conditions on other faces. On the 110 face the original charge distribution is approximated by a pyramid with a rectangular base,  $2r_1 \times 2r_2$ , the same that is formed on the  $s$ -polyhedron, Fig. 8. Its height is again such that the pyramid has the same volume as the segment cut off from the polyhedron. The charge distribution used for calculation of the kinetic energy is essentially the same as (12). For computing the potential energy we have now

$$\rho = M \cos \frac{\pi z}{2r_1} \cos \frac{\pi y}{2r_2} \pi e^{-\alpha/|x|} + N \pi \alpha e^{-\alpha/|x|} \operatorname{sgn} x \quad (20)$$

and

$$-\frac{V}{4\pi} = M \cos \frac{\pi z}{2r_1} \cos \frac{\pi y}{2r_2} \frac{1/\lambda}{\alpha^2 - \pi^2 \lambda^2} (\alpha e^{-\pi \lambda/|x|} - \pi \lambda e^{-\alpha/|x|}) + N \frac{\pi}{\alpha} (1 - e^{-\alpha/|x|}) \operatorname{sgn} x \quad (21)$$

with  $\lambda = (r_1^2 + r_2^2)^{1/2} / 2r_1 r_2$ , which can be also expressed in an integral form like (15). The charge has the pattern shown in Fig. 12(b) where the dots represent high negative charge for  $x > 0$  and low positive for  $x < 0$  and the circles indicate just the opposite. We have the kinetic energy

$$\text{K.E.} = -\sigma^{5/3} \frac{A}{\alpha} r_1 r_2 2.994 + \sigma B \alpha r_1 r_2 (1 + 2\lambda^2 W^2) 4 \ln 2 \quad (22)$$

with  $W = r_1 \beta_1 = r_2 \beta_2$  and the potential energy

$$\text{P.E.} = \frac{e^2 \sigma^2}{\alpha} \frac{2\alpha + k}{(\alpha + k)^2} \frac{r_1 r_2}{2\lambda} [1 + e^{\alpha c} (e^{\alpha c} - 2)] + \frac{e^2 \sigma^2}{\alpha^3} \frac{2r_1 r_2 k}{\lambda} \quad (23)$$

Differentiation gives again two equations for the minimum problem from which one obtains  $\alpha$  and  $W$ .

On the 100 face we have a pyramid with a square base. Thus all the formulas for the 110 face are valid if we put  $r = r_1 = r_2$ . The most complicated case is that of the 111 face. Here the charge distribution is symmetrical around a threefold axis. The actual shape of the segment of the  $s$ -polyhedron cannot be approximated as well as in the other cases. A pyramid with the triangular base seems to be the best choice. The edge of the base has the length  $d\sqrt{2}$  where  $d$  is the lattice constant. We have

$$\rho = M(\sin 2\pi z + 2 \sin \pi z \cos \pi y \sqrt{3}) \pi e^{-\alpha/|x|} + N \pi \alpha e^{-\alpha/|x|} \operatorname{sgn} x \quad (24)$$

and

$$-\frac{V}{4\pi} = M(\sin 2\pi z + 2 \sin \pi z \cos \pi y \sqrt{3}) \frac{1}{2(\alpha^2 - 4\pi^2)} (\alpha e^{-2\pi/|x|} - 2\pi e^{-\alpha/|x|}) + N \frac{\pi}{\alpha} (1 - e^{-\alpha/|x|}) \operatorname{sgn} x, \quad (25)$$

which can also be expressed in integral form. The charge pattern in the plane  $P$  is given in Fig. 12(c). We have the kinetic energy

$$\text{K.E.} = -\sigma^{5/3} \frac{A}{\alpha} h^2 \sqrt{3} 0.765 + \sigma B \alpha (h^2 + 9W^2) \frac{4}{3} \sqrt{3} \ln 2 \quad (26)$$

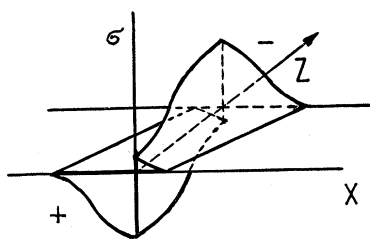


FIG. 11. Positive and negative charge distribution on the 211 face as used in the evaluation of the potential energy.

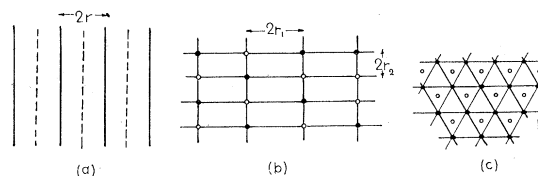


FIG. 12. Charge patterns on different faces of a body-centered lattice. Thick lines (or dots) indicate high negative or low positive charge density; dotted lines (or circles) indicate the opposite.

and the potential energy

$$\text{P.E.} = \frac{e^2 \sigma^2}{\alpha} \frac{\alpha + k}{(\alpha + 2k)^2} \frac{4\sqrt{3}}{27} h^3 [1 + e^{\alpha c} (e^{\alpha c} - 2)] + \frac{e^2 \sigma^2}{\alpha^3} \frac{2\sqrt{3}}{3} h^3 k \quad (27)$$

with  $k = \pi\sqrt{6}/3d$  and  $h = d\sqrt{6}/2$ . Differentiation of the total energy with respect to  $W$  and  $\alpha$  leads to the equations of the minimum problem.

The solution of the minimum problem for each of the faces of a crystal gives the final charge distribution. From this we know the values of the effective double layers and thus also the differences between the work functions for different crystal faces. Finally having the expressions for the total energy for each surface we can calculate the energy of formation of a certain surface. Or rather, since we have only the relative values, we get the differences between the surface energies of a crystal. The following is an application of all these considerations in a particular case.

### 5.

The first thing one has to know in order to apply the formulas developed above is the average density of electrons ( $n$  or  $\sigma$ ) which are involved in the formation of the double layer. In most cases this task is not easy. Among the metals for which data on work function are pretty well known only for sodium is this density accurately known. For other metals its estimate is more difficult. We are most interested in tungsten since the anisotropy for this metal is well measured. According to the calculations of Manning and Chodorow<sup>11</sup> there is much less than one electron per atom in the  $s$  band in metallic tungsten. On the other hand some of the  $d$  electrons might contribute to the effective density.

With the lattice constant of tungsten  $d = 3.16\text{\AA}$  we get for the different magnitudes appearing in our formulas the values, in angstrom units given in Table I. As mentioned above, the only magnitude which is not known is the electron density  $\sigma$ . For the minimum problem we assume one electron

<sup>11</sup> M. F. Manning and M. I. Chodorow, Phys. Rev. **56**, 787 (1939).

per atom. This value has not much justification for tungsten but is probably true for most of the monovalent metals. The equations of the minimum problem were solved for each surface separately by the trial and error method. In most cases it was sufficient to try a few neighboring values in the full equation and to interpolate. The results are given in Table II. We see first of all that  $\alpha$ , which is the parameter of the spreading of the charge in the direction normal to the surface, is almost constant. This is an interesting result and it justifies the point of view expressed in Part 1 that the positive contribution to the work function caused by the spreading is isotropic. Its value depends to a certain extent upon the analytical form of the charge distribution assumed in Eq. (12). It follows thus that all anisotropy is due to the smoothing of the charge distribution and formation of the new equilibrium surface. The magnitude  $W$ , given in Table II is the deviation of the surfaces of equal charge density, in the final distribution from the ideal plane  $P$ , see Fig. 2. We see that the conditions are very different on different surfaces; the 110 is smoothest, the 111

is the most rough. This result was qualitatively to be expected on the basis of comparison of the number of close-packed atoms in these surfaces. The last column shows what fraction of the charge  $Q_0$  which originally was outside of the plane  $P$  still remains outside in the form of the roughness  $Q_f$  of the surface and is not "smoothed out." Here we see again a great difference between the surfaces. In particular the difference between 211 and 100 should be noted since it is an essential point in the comparison with experiment, as made below.

Knowing the final charge distribution we can calculate the contributions to the double layers caused by spreading and smoothing of the charge. The first as we saw is almost isotropic and its value does not play a role in our comparison with experiment. However, we can use Bardeen's calculations, discussed in reference 1 and apply his result that the spread is about half the radius of the  $s$ -sphere. This result, obtained by more rigorous quantum-mechanical methods for a particular case is probably more correct than ours. This gives, with the help of formula (2),  $D \cong 1.2$  ev as the positive contribution to the work function under the assumption of one electron per atom.

The negative contributions to the work functions caused by smoothing are calculated first for the case of a perfectly smooth charge distribution, i.e., for  $\beta=0$ . Formulas (7)–(10) give with  $n=2$  and  $b=6a_0$  the values in the second column of Table III. These values are undoubtedly too high since the total work function for tungsten is about 4.5 ev. This is a result of our assumption of one electron per atom and  $\beta=0$ . It may be pointed out that  $\beta=0$  gives us the sequence of crystal faces in the order of decreasing work function: 110, 100, 211, 111. This is not in accord with experiment. We shall see that it is the correction due to  $\beta \neq 0$  which brings about the right sequence. The values of

TABLE I. Values of various constants for tungsten.

	110	211	100	111
$r$	$r_1=0.79$ $r_2=1.116$	1.116	1.116	$h=3.87$
$a$	1.116	1.935	1.580	1.824
$a_{\text{eff}}$	1.396	2.185	2.765	3.19

TABLE II. Parameters of the final charge distribution for tungsten.

SURFACE	$\alpha$	$W$	$Q_f/Q_0$
110	$1.10\text{\AA}^{-1}$	0.106A	0.15
211	1.08	0.600	0.55
100	1.10	0.518	0.37
111	1.14	0.910	0.46

the second column must be decreased by the contribution of charge which did not take part in the smoothing process. In Fig. 9 the dotted lines indicate how much charge is left over after the equilibrium distribution is established. The particularly simple dependence of  $\rho$  on distance from the plane  $P$  is of course the result of our approximations. It has no appreciable influence however on the results. In an actual crystal the contours are more smooth, the amount of displaced charge being practically the same.

From Table II we have the necessary data and with the help of formula (4) we can calculate the corrections. These corrected values in which the remaining unevenness of the charge distribution is taken into account are given in the third column of Table III. We see that the sequence of the faces is: 110, 211, 100, and 111. This is in accord with the experimental results of Nichols.<sup>1</sup> It may be mentioned here that there were attempts to explain the anisotropy of the work function relating it directly to the surface density of the atoms. This density relation however gives the same in correct sequence of faces, which was obtained for  $\beta=0$ . It appears thus that it is necessary to take into account the relative position of the atoms and the equilibrium distribution of charge in order to explain the observed facts.

Another comparison with experiment is the actual numerical value of the differences between the work function in different directions. Using  $V_{\beta \neq 0}$  from Table III and comparing with the last column in which the experimental data of Nichols are given, we see that the theoretical values are about six times too large. This is, in the first place, a result of the arbitrarily assumed density of one electron per atom, which is certainly too high. The only indication is the quoted result<sup>11</sup> that the density in the  $s-p$  band is of the order 0.1 electron per atom. We take here one-sixth of an electron per atom so as to

TABLE III. Contributions to work functions.

SURFACE	$V_{\beta=0}$	$V_{\beta \neq 0}$	$\Delta V_{\text{calc}}$	$\Delta V_{\text{obs}}$
110	0.44 ev	0.43 ev	0.38 ev	> 0.30 ev
211	2.04	1.35	0.22	0.30
100	1.64	1.40	0.21	0.17
111	3.48	2.70	0.0	0.0

fit the experimental data. The values  $\Delta V_{\text{calc}}$  given in the column before last in Table III are obtained by making use of the fact that the electron density is a linear factor in our expressions of the double layer. This statement is not quite true, however, for the minimum problem which depends on the charge density in a non-linear manner. It was checked, however, that the dependence of  $W$  upon electron density justifies this approximation. Both  $W$  and  $\alpha$  decrease slowly with decreasing  $\sigma$ . We see that the agreement between the computed and observed values is satisfactory in view of the simple model on which our theory is based.<sup>12</sup>

One important fact must be pointed out. All these computations were done as if the electronic charge density were uniform throughout the crystal, i.e., as if the ion cores were small. This may be a good approximation in the case of sodium but is less good for tungsten. Studies of the structure of the electron bands in metallic tungsten indicate that the  $6s$  and  $5d$  bands are broad and overlap considerably. About one-third of the four  $d$  electrons in an atom lie outside of the metallic  $s$ -sphere. Thus the ionic core is large and even the lower energy states are perturbed. It follows that a deformation of the original spherically symmetric charge distribution involves an additional potential energy. This is true especially for deep-penetrating

<sup>12</sup> The  $\Delta V$  are calculated with respect to the 111 rather than to the 110 plane. This is more satisfactory since the observed work function on the 110 plane is probably too low by 0.1 ev or more (see M. Nichols reference 1).

TABLE IV. Energy per unit area; ergs/cm<sup>2</sup>.

Surface	110	211	100	111
Energy	30	334	362	952

disturbances. One might expect thus that the smoothing is less complete than would follow from our theory. As a result the negative contributions to the work function would be somewhat smaller than those in Table III.

Finally as indicated before, we can calculate the total energy per unit area for each of the four surfaces. From formulas (13), (17), (22), (23), (26), (27), we obtain the energy in ergs per cm<sup>2</sup> as given in Table IV. This is not the actual surface energy since in tungsten we might expect most of the binding energy to be due to the  $5d$  electrons<sup>13</sup> which as mentioned above extend near to the surface of the  $s$ -spheres. However, these figures give the relative expenditure of energy in formation of these surfaces. We see that the most stable is the 110 face and the least stable the 111 face. These results agree with the observations on single crystals of tungsten. In particular the stability and development of the 110 and 211 faces is in accord with experimental data. Since the values in Table IV are differences of numbers of the order of about 2500 the relative error for the 110 face is large. On the other hand for the 111 face the approximation of the uniform charge distribution is least satisfactory since here the deeper layers around the atom are disturbed. Therefore these two extreme cases are less certain.

The author takes the opportunity to express his sincere thanks to Professor E. Wigner for advice and helpful criticism, and to Dr. C. Herring and Dr. M. Nichols for valuable discussion and remarks.

<sup>13</sup> See F. Seitz, reference 8, p. 432.